A Millimeter Wave Testbed for Repeatable High Velocity Measurements

Erich Zöchmann[†], Robert Langwieser[†], Sebastian Caban[†], Martin Lerch[*†],
Stefan Pratschner[*†], Ronald Nissel[*†‡], Christoph F. Mecklenbräuker[†‡], and Markus Rupp[†‡]
[*] Christian Doppler Laboratory for Dependable Wireless Connectivity for the Society in Motion
[†] Institute of Telecommunications, TU Wien, Austria
[‡] Department of Radio Electronics, TU Brno, Czech Republic
ezoechma@nt.tuwien.ac.at

***Abstract*—Future applications of millimeter waves (mmWaves) in vehicular scenarios ask for the characterization of the time-variant wideband mmWave channel. For this contribution, we manufactured and measured a proof of concept circuitry intended to receive mmWave signals repeatably at velocities of up to 50 meters per second (=180km/h=112mph). Our design is based on a rotating arm, spinning a small antenna platform around a central pivot in a repeatable manner. Two single-channel rotary joints are used for interfacing multiplexed I and Q components, auxiliary carriers, as well as the DC power supply to and from the small antenna platform at the end of the spinning arm. Our custom designed RF circuitry withstands the accelerations caused by centripetal forces of up to 250g. Measurements of scattering parameters and phase noise show the applicability of our design.**

I. Introduction

A. Importance and Prior Work

Millimeter Wave (mmWave) automotive radars are a mature technology [1]. mmWave frequencies are considered for future mobile communication systems and the authors of [2] consider them for vehicular communications too. Current vehicular communications takes place at much lower frequencies and with relatively small bandwidths. Channel characterizations and their implications can be found in [3], [4]. At mmWave frequencies, the fusion of radar systems, communication systems [5], and large bandwidths is very attractive. Cars can increase their sensing range by fusing their sensor data with data from infrastructure or other cars by means of ad-hoc mmWave links [2]. Future trains will have improved mobile access [6] and the authors of [7] even predict mmWaves as well as THz communications as access technology. Speaking generally, we will see a whole (mmWave) connected society in motion [8].

The static mmWave radio channel for example at $60\,\mathrm{GHz}$ is well investigated [9]–[13] and signal processing algorithms are at hand [14], [15]. There is hardly any knowledge about rapidly changing radio channels, albeit the theoretical work of [16] links the angular power distribution results from static channels with omnidirectional Doppler spectra for moving receivers. During the development phase of algorithms, a controllable experiment with reproducable outcome is indispensable for proper cross-comparison. Repeatable [17] linear movements, by means of linear guides, are feasible only for low velocities [18], unless very long guides are used. A solution to enable repeatable, high velocity measurements is to spin an antenna (platform) around a central pivot. The measurements are then conducted on a small segment of the circumference, thereby emulating linear translations. Such an approach has been used for the evaluation of LTE in [19]–[23].

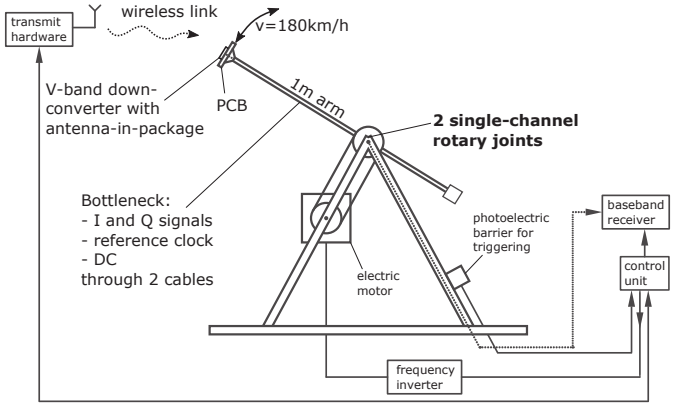

Fig. 1. The high velocity testbed proposed to examine, for example, vehicular to infrastructure communications. For $50\,\mathrm{m/s}$ circumferential speed, the acceleration caused by the centripetal forces at the end of the arm is roughly $250\,g$.

This design inherently relies on rotary joints to interface all signals coming from or to the end of the arm, see Fig. 1. For an $1\,\mathrm{m}$ long arm and an antenna velocity of $112\,\mathrm{mph} = 180\,\mathrm{km/h}$, the rotary joints must withstand approximately 500 revolutions per minute. Using off-the-shelf components, this limits us to single-channel (coaxial) rotary joints, one on either side of the pivot. Transmitting mmWave signals directly through rotary joints and $2\,\mathrm{m}$ long cables leads to losses ($> 15\,\mathrm{dB}$) and phase instabilities. We thus propose to convert the mmWave signal to low IF or baseband, directly at the antenna at the end of the arm.

B. Our contribution

We propose the set-up in Fig. 1 which uses two single-channel rotary joints and conversion to baseband. It allows for repeatable high velocity, time-variant mmWave links mea-

surements. It requires a triplexer at the PCB, that withstands high g-forces. A proof of concept prototype was manufactured, measured, and compared against simulation.

II. Circuit Concept

For the demonstration of our concept, we work with a commercial off-the-shelf V-band radio frequency integrated circuit from Hittite. This IC that includes the antenna-on-chip was characterized in [24]. These down-converters and up-converters are also available as flanged modules from [25]. We used the flanged modules for our back-to-back measurements in Section IV.

In this paper, without loss of generality, we focus our concept on a moving receiver. The down-converter IC HMC6001LP711E receives a $1.8\,\mathrm{GHz}$ wide V-band signal within $57\,\mathrm{GHz}$ to $64\,\mathrm{GHz}$ and converts it to in-phase and quadrature-phase. For the internal synthesizer Phase-Locked Loop (PLL), a reference clock of $285.714\,\mathrm{MHz}$ is needed. Furthermore control signals and DC power supply have to be applied to the IC.

Because our set-up is constrained by two single-channel rotary joints, we need a solution to transfer I and Q signals, the reference clock, the control signals, and DC from and to the V-band IC. It is not possible to generate the reference clock directly on the accelerated PCB since quartz oscillators de-tune at high g-forces. As the reference clock frequency lies inside the I and Q spectra, we decided to transfer this reference clock above the baseband spectrum in form of two auxiliary carriers, separated by the reference clock frequency. As illustrated in Fig. 2, the full circuit composes of four parts:

1) Auxiliary carrier generation: By mixing a $2.433\,\mathrm{GHz}$[1] auxiliary carrier with the reference clock of $285.714\,\mathrm{MHz}$, we obtain a second auxiliary carrier at $2.147286\,\mathrm{GHz} \approx 2.15\,\mathrm{GHz}$. Only those two auxiliary carriers are passed to the next stage.

2) Two triplexing stages:
   a) The in-phase receive baseband signal, the $2.433\,\mathrm{GHz}$ auxiliary carrier and V_{DC1} and
   b) the quadrature-phase receive baseband signal, the $2.15\,\mathrm{GHz}$ auxiliary carrier and V_{DC2}

   are combined onto either transmission line. The resulting signals are transmitted through two single-channel rotary joints to the stages in motion.

3) Two single-channel rotary joints

4) Rotated receiver PCB: We need two triplexers to separate the receive signals, the auxiliary carriers, and DC. These triplexers need to withstand acceleration forces of more than $200\,g$, see Fig. 1. Details to the triplexers are given in Section III. The two auxiliary carriers are fed into a mixer to recover the reference clock. Eventually, the upper sideband and carrier leakages are filtered out with a differential lowpass filter.

[1] A high quality LO at this frequency was readily available. Note that this frequency lies sub-optimally within an ISM band.

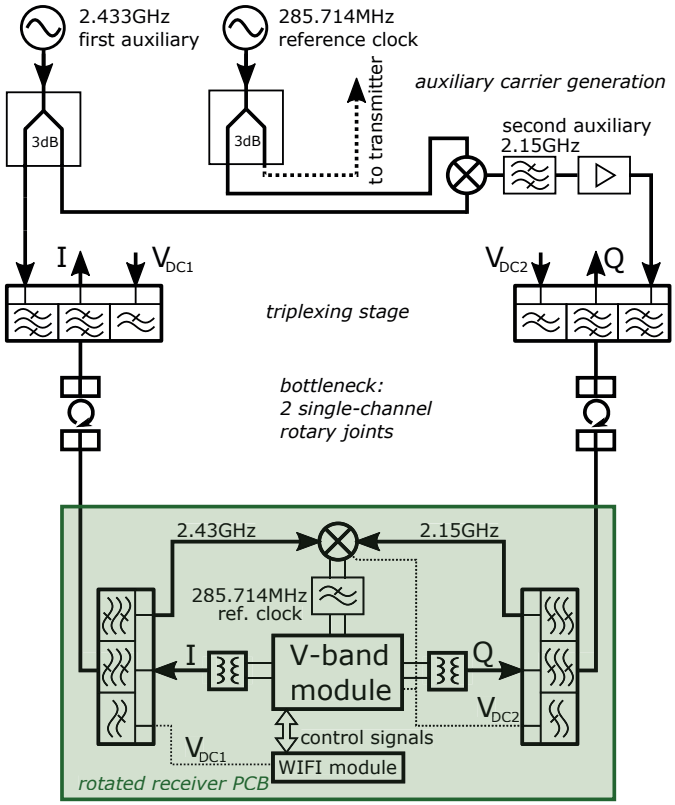

Fig. 2. Frequency multiplexing concept to circumvent the two single-channel rotary joint bottleneck. The auxiliary carrier generation is performed with a mixing stage to be able to share the reference clock with the transmitter.

We use a WIFI module (ESP8266) to configure the V-band module while the receiver is not rotating. During the measurements the WIFI module is powered down by disconnecting its separated DC supply.

III. PCB and Triplexer Design

To keep microstrip lines reasonable narrow, the PCB needs to be thinner than $0.3\,\mathrm{mm}$. But, for mechanical stability (drag, vibrations, and acceleration), the PCB must be thick and without RF shielding. To fulfil those requirements at fair costs, we designed our prototype on a 4-layer FR4 substrate. The pre-pregs are $0.28\,\mathrm{mm}$ and the core is $0.71\,\mathrm{mm}$.

For mechanical reasons, we mounted all components, except for the V-band module with the antenna-on-chip, at the bottom side (g-force towards the PCB). Nevertheless, a just $10\,\mathrm{gram}$ heavy, off-the-shelf triplexer mounted on the PCB at the end of the rotated arm is subject to a force of $25\,\mathrm{N}$. We therefore decided to build a triplexer based on microstrip lines with as few lumped components as possible. Our approach is inspired by [26], where parallel coupled resonators were used.

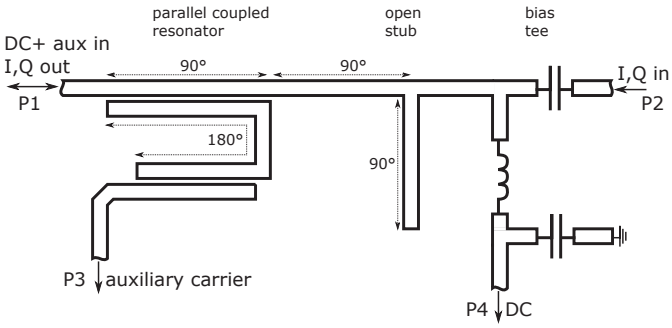

Fig. 3. The microstrip triplexer unit on the rotated PCB. The auxiliary carrier is coupled out via a very narrowband parallel coupled resonator structure.The electrical length of 90° or 180° translates to specific physical lengths for each auxiliary carrier frequency (2.15 GHz or 2.433 GHz).

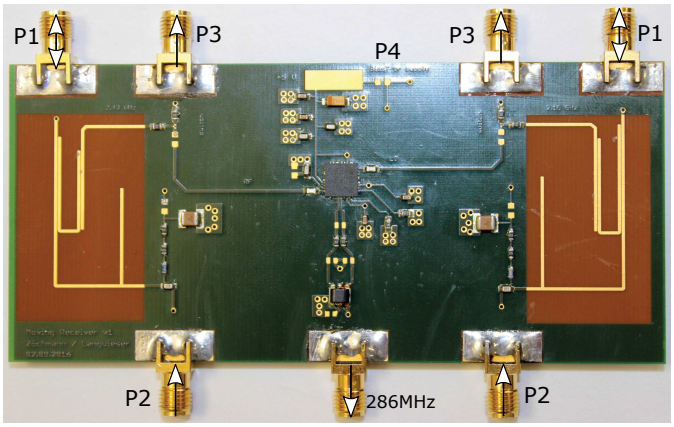

Fig. 4. Bottom side of the realized concept circuit. The areas without solder resist are the first two stages of the microstrip triplexers. Note the different sizes of the resonators, which are matched to the different auxiliary carriers. The mixer (MAX2043) is right in between the two triplexers.

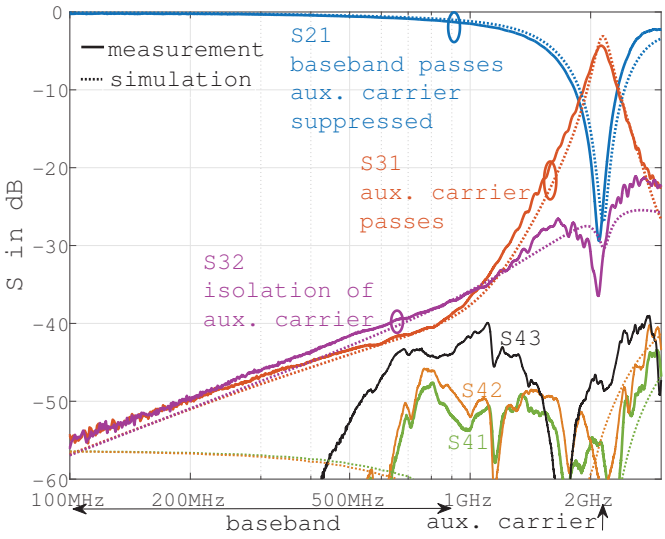

Fig. 5. All transmission parameters of the manufactured prototype with resonator frequency of 2.15 GHz. Note that the passband of the DC path is not visual on a log-scale frequency axis.

The design is broken up into three stages, see Fig. 3. The first two stages, namely the parallel coupled resonator and the open stub notch filter, follow the design proposal of [26]. Without the strong auxiliary carrier suppression of the notch filter, the V-band module's output is potentially been driven non-linear. Furthermore, our design is deliberately made narrowband to increase the decoupling between frequency bands. This supports the removal of leakages and products of non-linearities from the preceding mixing stage. To increase the coupling efficiency, the coupler is $90°$ in electrical length. The $\lambda/2$ parallel coupled resonator is bended to save space. The resonator is exactly tuned to the auxiliary carrier to be coupled out. The distance to the subsequent open stub is matched, such that constructive coupling of the reflected wave is achieved. The third frequency branch - the DC path - is realized as a bias tee. Note that the DC blocking capacitor is attenuating the low frequency components of I and Q.

The manufactured FR4-PCB is presented in Fig. 4. In Fig. 5, the "AWR Microwave Office" simulation results for the 2.15 GHz triplexer are shown in dashed lines and compared to the measurements in solid lines. The second triplexer, with the 2.433 GHz resonator, has slightly better isolation.

IV. Measurements Including Baseband Hardware

The previous measurements were characterising the triplexer. To characterize the testbed performance, we need to introduce the baseband hardware around the rotary unit. Already in Fig. 1, the necessary units are sketched. The whole testbed is schematically shown in Fig. 6. Similar to the approach in [27], waveforms are generated off-line for example in MATLAB, digitally up-converted to an Intermediate Frequency (IF) and transmitted by an Arbitrary Waveform Generator (AWG) who acts as Digital-to-Analog Converter (DAC) for transmitting signals in in-phase and quadrature-phase. Those signals are up-converted to the V-band by an external mixer with built-in synthesizer PLL. The PLL is locking on a reference clock of 285.714 MHz and is capable of synthesizing a frequency grid of $\Delta f = \frac{7}{4}\,285.714\,\text{MHz} \approx 500\,\text{MHz}$ distance. To avoid IF crosstalk, we operate the transmitter and the receiver at different IFs. Furthermore, the mirror frequencies are suppressed as the Local Oscillator (LO) at the receiver is Δf higher than the LO at the transmitter, see [13].

Besides the ADC, the receiver baseband hardware comes with a triggering unit to guarantee time-synchronization [28]. Furthermore, the control unit at the receive side is responsible for processing the signal from the photoelectric barrier and for setting the frequency inverter to control the velocity of the electric motor. After a pulse of the photoelectric barrier was applied, a trigger is generated. Thereby, different kind of transmit waveforms are transmitted and received every time at the exactly same position. This unit is reused from our 2.5 GHz testbed, see details in [29]–[31]. The reference clock is shared among the transmitter and receiver. To prevent any

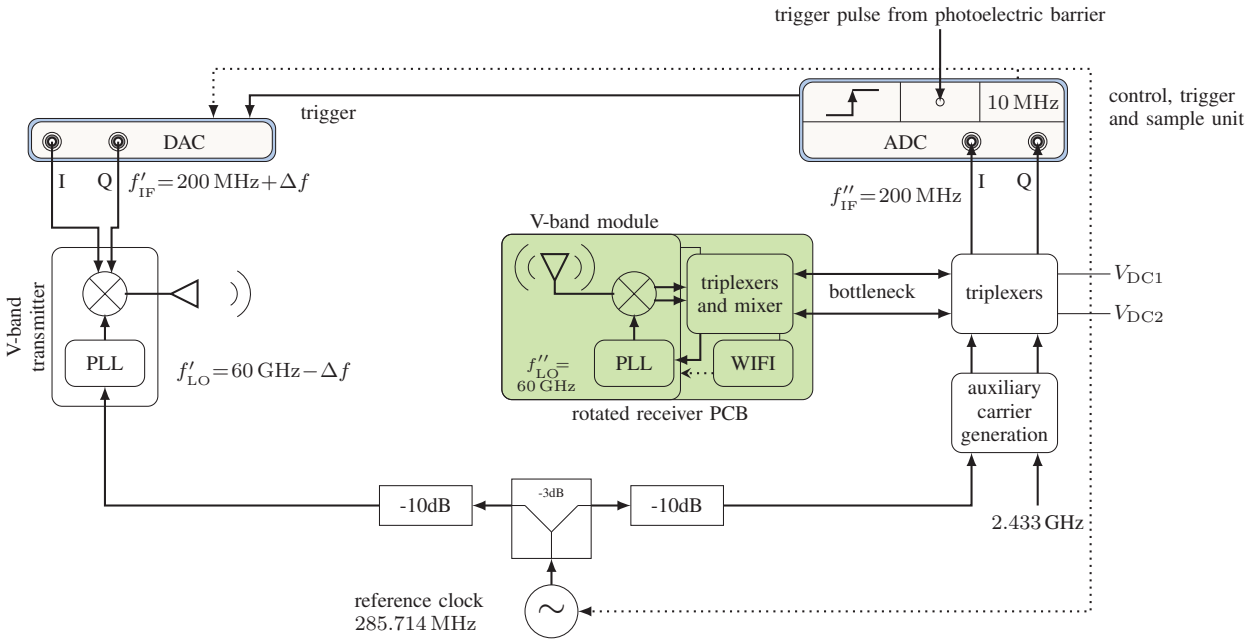

Fig. 6. Interaction of the rotated receiver PCB with the baseband hardware. The baseband hardware consists of fast sampling DACs and ADCs to enable a software defined radio approach. Any kind of waveform which fits into 1 GHz of baseband spectrum can be transmitted.

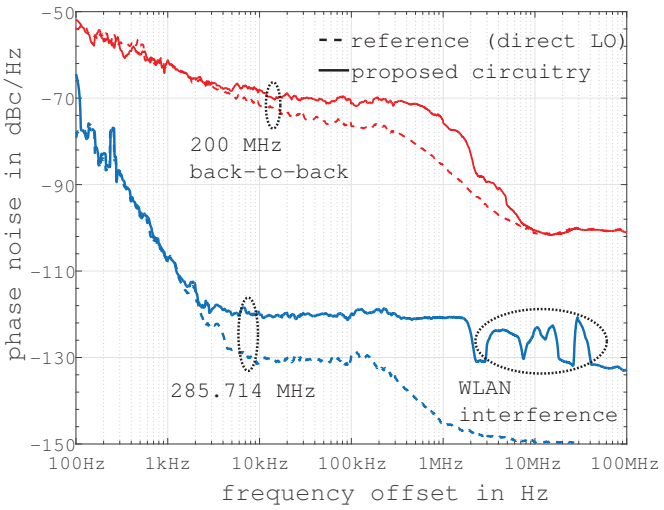

Fig. 7. Measured phase noise performance. Besides the increased phase noise due to mixing of the auxiliary carriers, there is also WLAN interference visual. The upper curves reflects the impact of the circuit for V-band performance.

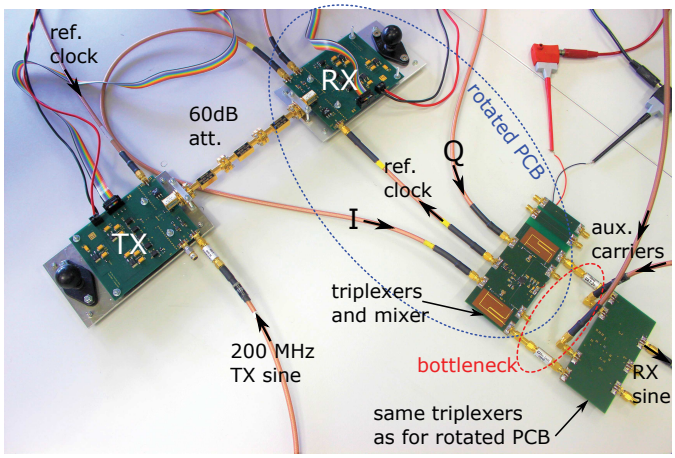

Fig. 8. Back-to-back configuration to access the phase noise performance off V-band transmissions. The transmitter is connected via 60 dB attenuation with the receiver. The reference clock is generated via the proposed multiplexing set-up.

RF leakage via the clock cables, the power splitter isolation of 25 dB and is further increased by additional attenuators.

From Fig. 6, it should become clear, that the developed triplexer-mixer circuitry should act as a transparent interface for the single-channel rotary joint bottleneck. To test the impact of the mixing circuits on our set-up, we measure the phase noise performance. Phase noise is a key aspect for time-variant wireless channel measurements as Doppler spectra below the phase noise level are not visual [32].

Our measurement results are shown in Fig. 7. We first compare the quality of the reference clock generated with our circuitry to an ideal reference. The results are shown in blue in Fig. 7. Due to the coherent generation of the auxiliary carriers and the mixing circuit on the rotated PCB for recovering the reference clock, we see an increased phase noise level. As the first resonator, tuned for 2.433 GHz, lies within an ISM band we can observe WLAN interference as well. Remember, we are able to turn off our WIFI module by its separated DC supply.

Next, to assess the impact on the actual V-band transmissions, we connected the transmit and receive module back-to-back via 60 dB attenuation, see Fig. 8. The phase noise of a 200 MHz sine wave, transmitted over a 60 GHz link, was compared, once by applying the ideal reference clock directly to the receive module, and once via the proposed multiplexing-mixing circuit. The decreased reference clock performance becomes visual for 60 GHz transmissions.

V. Conclusion

We proposed repeatability of time-variant, high velocity mmWave experiments by circular motion. Received mmWave signals are downconverted locally at the antenna platform and interfaced to a static baseband receiver through rotary joints. A proof of concept prototype was manufactured and measured. Our approach trades off phase noise performance with repeatability.

Acknowledgment

The financial support by the Austrian Federal Ministry of Science, Research and Economy and the National Foundation for Research, Technology and Development is gratefully acknowledged. The research has been co-financed by the Czech Science Foundation, Project No. 17-18675S "Future transceiver techniques for the society in motion", Project No. 17-27068S "Mobile channel analysis and modelling in millimeter wave band", and by the Czech Ministry of Education in the frame of the National Sustainability Program under grant LO1401.

References

[1] M. E. Russell, A. Crain, A. Curran, R. A. Campbell, C. A. Drubin, and W. F. Miccioli, "Millimeter-wave radar sensor for automotive intelligent cruise control (ICC)," *IEEE Transactions on Microwave Theory and Techniques*, vol. 45, no. 12, pp. 2444–2453, 1997.

[2] V. Va, T. Shimizu, G. Bansal, and R. W. Heath Jr, "Millimeter wave vehicular communications: A survey," *Foundations and Trends® in Networking*, vol. 10, no. 1, pp. 1–113, 2016.

[3] A. Paier, J. Karedal, N. Czink, C. Dumard, T. Zemen, F. Tufvesson, A. F. Molisch, and C. F. Mecklenbräuker, "Characterization of vehicle-to-vehicle radio channels from measurements at 5.2 GHz," *Wireless personal communications*, vol. 50, no. 1, pp. 19–32, 2009.

[4] C. F. Mecklenbräuker, A. F. Molisch, J. Karedal, F. Tufvesson, A. Paier, L. Bernadó, T. Zemen, O. Klemp, and N. Czink, "Vehicular channel characterization and its implications for wireless system design and performance," *Proceedings of the IEEE*, vol. 99, no. 7, pp. 1189–1212, 2011.

[5] C. Sturm, T. Zwick, and W. Wiesbeck, "An OFDM system concept for joint radar and communications operations," in *Proc. of IEEE Vehicular Technology Conference (VTC Spring)*, 2009, pp. 1–5.

[6] M. K. Müller, M. Taranetz, and M. Rupp, "Providing current and future cellular services to high speed trains," *IEEE Communications Magazine*, vol. 53, no. 10, pp. 96–101, 2015.

[7] K. Guan, G. Li, T. Kürner, A. F. Molisch, B. Peng, R. He, B. Hui, J. Kim, and Z. Zhong, "On millimeter wave and THz mobile radio channel for smart rail mobility," *IEEE Transactions on Vehicular Technology*, 2016.

[8] S. Schwarz and M. Rupp, "Society in motion: Challenges for LTE and beyond mobile communications," *IEEE Communications Magazine*, vol. 54, no. 5, pp. 76–83, 2016.

[9] S. Geng, J. Kivinen, X. Zhao, and P. Vainikainen, "Millimeter-wave propagation channel characterization for short-range wireless communications," *IEEE Transactions on Vehicular Technology*, vol. 58, no. 1, pp. 3–13, 2009.

[10] P. F. Smulders, "Statistical characterization of 60-GHz indoor radio channels," *IEEE Transactions on Antennas and Propagation*, vol. 57, no. 10, pp. 2820–2829, 2009.

[11] S. Ranvier, J. Kivinen, and P. Vainikainen, "Millimeter-wave MIMO radio channel sounder," *IEEE Transactions on Instrumentation and Measurement*, vol. 56, no. 3, pp. 1018–1024, 2007.

[12] N. Moraitis and P. Constantinou, "Measurements and characterization of wideband indoor radio channel at 60 GHz," *IEEE Transactions on Wireless Communications*, vol. 5, no. 4, pp. 880–889, 2006.

[13] E. Zöchmann, M. Lerch, S. Caban, R. Langwieser, C. F. Mecklenbräuker, and M. Rupp, "Directional evaluation of receive power, Rician K-factor and RMS delay spread obtained from power measurements of 60 GHz indoor channels," in *Proc. of IEEE-APS Topical Conference on Antennas and Propagation in Wireless Communications (APWC)*, Cairns, Australia, 2016.

[14] E. Zöchmann, S. Schwarz, and M. Rupp, "Comparing antenna selection and hybrid precoding for millimeter wave wireless communications," in *Proc. of IEEE Sensor Array and Multichannel Signal Processing Workshop (SAM)*, Rio de Janeiro, Brazil, 2016.

[15] R. Méndez-Rial, C. Rusu, N. González-Prelcic, A. Alkhateeb, and R. W. Heath, "Hybrid MIMO architectures for millimeter wave communications: Phase shifters or switches?" *IEEE Access*, vol. 4, pp. 247–267, 2016.

[16] E. Zöchmann, S. Caban, M. Lerch, and M. Rupp, "Resolving the angular profile of 60 GHz wireless channels by delay-Doppler measurements," in *Proc. of IEEE Sensor Array and Multichannel Signal Processing Workshop (SAM)*, 2016, pp. 1–5.

[17] M. Lerch, S. Caban, E. Zöchmann, and M. Rupp, "Quantifying the repeatability of wireless channels by quantized channel state information," in *Proc. of IEEE Sensor Array and Multichannel Signal Processing Workshop (SAM)*, Rio de Janeiro, Brazil, 2016.

[18] S. Caban, J. Rodas, and J. A. García-Naya, "A methodology for repeatable, off-line, closed-loop wireless communication system measurements at very high velocities of up to 560 km/h," in *Proc. of IEEE Instrumentation and Measurement Technology Conference (I2MTC)*, 2011.

[19] J. Rodríguez-Piñeiro, M. Lerch, J. A. García-Naya, S. Caban, M. Rupp, and L. Castedo, "Emulating extreme velocities of mobile LTE receivers in the downlink," *EURASIP Journal on Wireless Communications and Networking*, vol. 2015, no. 1, pp. 1–14, 2015.

[20] J. Rodriguez-Pineiro, P. Suárez-Casal, M. Lerch, S. Caban, J. A. Garcia-Naya, L. Castedo, and M. Rupp, "LTE downlink performance in high speed trains," in *Proc. of Vehicular Technology Conference (VTC Spring)*. IEEE, 2015, pp. 1–5.

[21] M. Lerch, "Experimental comparison of fast-fading channel interpolation methods for the LTE uplink," in *Proc. of International Symposium ELMAR*, Zadar, Croatia, 2015.

[22] R. Nissel and M. Rupp, "Doubly-selective MMSE channel estimation and ICI mitigation for OFDM systems," in *Proc. of IEEE International Conference on Communications (ICC)*, London, UK, 2015.

[23] R. Nissel, M. Lerch, and M. Rupp, "Experimental validation of the OFDM bit error probability for a moving receive antenna," in *Proc. of IEEE Vehicular Technology Conference (VTC)*, Vancouver, Canada, 2014.

[24] P. Zetterberg and R. Fardi, "Open source SDR frontend and measurements for 60-GHz wireless experimentation," *IEEE Access*, vol. 3, pp. 445–456, 2015.

[25] "60 GHz transmitter and 60 GHz receiver modules." https://www.pasternack.com/60-ghz-modules-category.aspx, accessed: 2017-02-01.

[26] G. Matthaei and E. Cristal, "Multiplexer channel-separating units using interdigital and parallel-coupled filters," *IEEE Transactions on Microwave Theory and Techniques*, vol. 13, no. 3, pp. 328–334, 1965.

[27] R. Nissel, E. Zöchmann, M. Lerch, S. Caban, and M. Rupp, "Low-latency MISO FBMC-OQAM: It works for millimeter waves!" in *Proc. of IEEE International Microwave Symposium (IMS)*, Hawaii, USA, Jun 2017.

[28] S. Caban, A. Disslbacher-Fink, J. A. García-Naya, and M. Rupp, "Synchronization of wireless radio testbed measurements," in *Proc. of IEEE Instrumentation and Measurement Technology Conference (I2MTC)*. IEEE, 2011, pp. 1–4.

[29] M. Lerch, S. Caban, M. Mayer, and M. Rupp, "The Vienna MIMO testbed: Evaluation of future mobile communication techniques," *Intel Technology Journal*, vol. 18, pp. 58–69, 2014.

[30] S. Caban, C. Mehlführer, G. Lechner, and M. Rupp, "Testbedding MIMO HSDPA and WiMAX," in *Proc. of IEEE Vehicular Technology Conference (VTC-Fall)*, 2009, pp. 1–5.

[31] C. Mehlführer, S. Geirhofer, S. Caban, and M. Rupp, "A flexible MIMO testbed with remote access," in *Proc. of European Signal Processing Conference (EUSIPCO)*. IEEE, 2005, pp. 1–4.

[32] M. Lerch, E. Zöchmann, S. Caban, and M. Rupp, "Noise bounds in multicarrier mmWave Doppler measurements," in *Proc. of the European Wireless Conference (EW)*, Dresden, Germany, 2017, pp. 1–6.